Proc. Natl. Acad. Sci. USA
Vol. 90, pp. 1686–1690, March 1993
Ecology

Pulsed phytoplankton supply to the rocky subtidal zone: Influence of internal waves

(benthic–pelagic coupling/rocky subtidal benthos/suspension feeders)

JON D. WITMAN*†, JAMES J. LEICHTER*, SALVATORE J. GENOVESE*, AND DAVID A. BROOKS‡

*Marine Science Center, Northeastern University, Nahant, MA 01908; and ‡Department of Oceanography, Texas A & M University, College Station, TX 77843

Communicated by Robert T. Paine, September 14, 1992

ABSTRACT **Hydrographic measurements indicate that the thermocline and the phytoplankton-rich chlorophyll maximum layer are vertically displaced over a rocky pinnacle in the central Gulf of Maine by internal waves with maximum amplitudes of 27 m. Such predictable downwelling events are linked to rapid, 2- to 3-fold increases in chlorophyll *a*, an indicator of phytoplankton concentration, in pulses of warm water recorded 4 cm above the bottom (29-m depth). The 1.5–5.6°C temperature fluctuations had an average period of 10.6 min and were generated on both ebb and flood tides. Local lee waves and the arrival of solitons propagated from Georges Bank are hypothesized to explain the timing of the internal waves. Because internal waves and chlorophyll maxima are pervasive features of stratified temperate seas, this mechanism of food coupling should be common in other rocky subtidal habitats.**

Despite the long-acknowledged dependence of bottom-dwelling populations on pelagic processes (1), relatively little is known about how events in the water column influence organisms inhabiting rocky subtidal habitats along the underwater coastline of continents at high latitudes and on offshore ledges, banks, and seamounts. Recent benthic–pelagic coupling research has linked the impingement of an oxygen minimum layer (2) and topographically enhanced currents (3) to the vertical zonation of invertebrate communities on Pacific seamounts. The importance of understanding the process of food supply to the sea floor is underscored by the finding that the input of particulate organic carbon can regulate the size and distribution of populations in soft bottom habitats (4, 5). Moreover, the timing of phytoplankton supply is thought to influence the evolution of benthic invertebrate reproductive strategies (6).

Internal waves are generated when the ebb tide forces a shallow thermocline over the edge of a steep bottom feature such as a bank, ledge, or continental shelf (7). A prominent depression of the thermocline is produced on the downstream side and held over the abrupt bottom until the ebbing currents slacken. The released depression propagates away from the topographic feature as a packet of internal waves (8, 9). Because of their ability to move phytoplankton-rich chlorophyll maximum layers downward (10–12), internal waves are a likely mechanism of benthic–pelagic food coupling. To date, investigations of internal wave effects on phytoplankton distribution have been restricted to the water column, and it is not evident that downwelled chlorophyll maximum layers could reach the rough surface of rocky bottoms where topographically induced upwelling could redirect downward flow (13–15).

We studied benthic–pelagic coupling at Ammen Rock Pinnacle (ARP), a rocky ledge located 105 km offshore in the central Gulf of Maine characterized by steep bottom topography, swift currents (averages, 12.7–25.5 cm/sec) and abundant populations of suspension-feeding sponges, anemones, bryozoans, and ascidians (Fig. 1 and refs. 16 and 17). Observations of rapid vertical displacements of the subsurface chlorophyll maximum (SCM) layer (e.g., 20-m depth in 15 min) at ARP in July 1990 led us to hypothesize that internal waves deliver phytoplankton to deep habitats by displacing the SCM layer down to the bottom.

In this report, we describe the vertical extent of short-term temperature fluctuations associated with the passage of internal waves over ARP. We then show that the pulses of warm water are accompanied by large increases in chlorophyll *a*, signaling the arrival of the SCM layer on the bottom. Using thermistor string records, time series analysis, and photos from space, we develop the hypothesis that the internal waves arriving on the ebb tide are generated locally, while those arriving around the flood tide propagate away from Georges Bank.

The significance of this vertical coupling phenomenon lies in its potential to enhance the secondary productivity of suspension-feeding invertebrate populations living on topographically high regions of the sea floor. It may also serve as a vertical transport mechanism for passively dispersed larvae of benthic invertebrates, since bryozoan larvae are abundant in the SCM above offshore pinnacles (J.D.W., unpublished data). To our knowledge, this is the first evidence that physical forcing by internal waves extends all the way down to the substratum in the rocky subtidal zone.

METHODS

Most of the research was conducted at 29-m depth on a narrow, 37-m-long ridge at the peak of ARP (Fig. 1). Movements of the thermocline were followed in June and July 1991 by a vertical string of six thermistors MicroTemps (Coastal Leasing, Cambridge, MA) extending from the peak to a surface buoy. Temperature was measured once per minute. The SCM layer was tracked by vertical profiling with a conductivity/temperature/depth (CTD) instrument (model SBE-19, Sea Bird Electronics, Bellevue, WA) equipped with an *in situ* fluorometer (SeaTech, Corvallis, OR). To follow movements of the SCM near the bottom, the CTD/fluorometer was repeatedly moored to the top of the pinnacle so that the instrument sensors were ≈20 cm above the rock surface. Sampling rates were 2 Hz for the CTD and 5 Hz for the fluorometer. Data were smoothed and stored every 10 sec and subsequently averaged at 1-min intervals.

Rapid temperature fluctuations, on the order of 1.5–8.5°C in 2–15 min, were considered preliminary evidence of internal wave activity (18), while elevated levels of fluorescence

The publication costs of this article were defrayed in part by page charge payment. This article must therefore be hereby marked "*advertisement*" in accordance with 18 U.S.C. §1734 solely to indicate this fact.

Abbreviations: ARP, Ammen Rock Pinnacle; CTD, conductivity/temperature/depth; SCM, subsurface chlorophyll maximum.

†To whom reprint requests should be addressed.

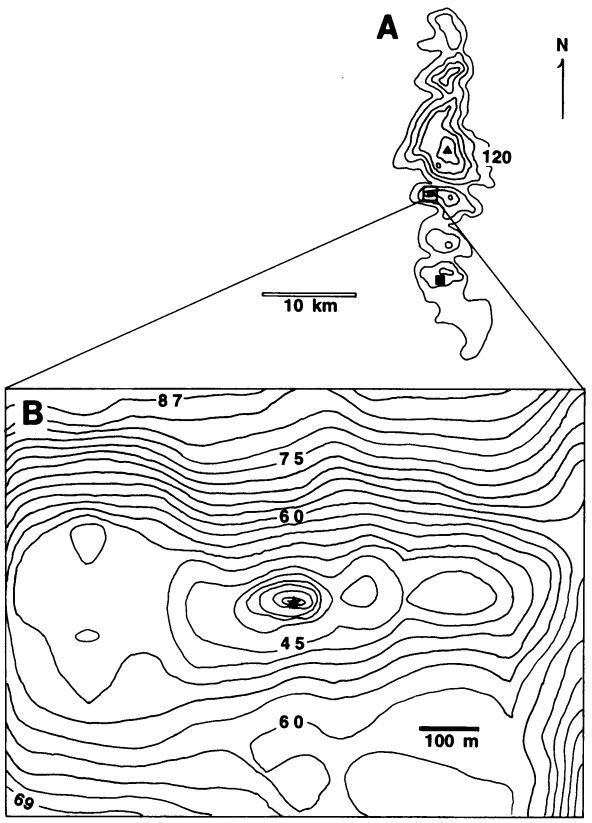

FIG. 1. (*A*) Bathymetry of Cashes Ledge, 105 km offshore in the central Gulf of Maine, showing the location of ARP (open square), where most of the research was conducted (42° 51′ 25″ N, 68° 57′ 11″ W). Depth contours are 20 m. A solid square marks the south Cashes site, where a thermistor string was deployed for comparison to ARP. Ammen Rock (solid triangle) is where lee waves are hypothesized to form. (*B*) Detailed bathymetry of the ARP site. The peak site (star) is an east–west trending ridge largely outlined by the 30-m isobath and is the site of repeated deployments of the CTD/fluorometer system, thermistor string, and current meters in June and July 1991.

recorded as chlorophyll *a* equivalents in the CTD bottom mooring configuration or in vertical casts identified the SCM layer. The calibration of fluorescence volts to chlorophyll *a* concentration in micrograms per liter was provided by SeaTech, manufacturer of the fluorometer. SeaTech fluorometers have provided highly accurate measurements of *in vivo* fluorescence (19). The manufacturers of the CTD (Sea Bird Electronics) and fluorometer (SeaTech) claim that the analog/digital circuitry interfacing the two instruments is unaffected by temperature changes and that the fluorometer is temperature-compensated. The SCM layer corresponds to a phytoplankton abundance maximum in the Gulf of Maine (20, 21).

Spectral analysis was conducted on the July 22–29 bottom temperature record to discern the frequency of the arrival of internal wave packets. The analytical procedure consisted of filtering the high-frequency noise by averaging the 9000-min temperature file at 16-min intervals, then detrending the data for a significant low-frequency trend of warmer mean temperature during the latter half of the week. Detrending consisted of subtracting from the raw data a smoothed curve fit to a third-order polynomial which yielded a better fit than a linear function. Fast Fourier transforms were computed on the filtered, detrended data to reveal the spectral peaks.

RESULTS AND DISCUSSION

Vertical Coupling. The CTD/fluorometer moored 20 cm above the rock surface showed rapid temperature fluctuations of 1.5–5.6°C amplitude commonly occurring at the peak of ARP during 105 and 125 hr of deployment in June and July, respectively (Fig. 2). The bottom thermistor of the vertical string, located 10 m horizontal distance from the CTD/fluorometer, recorded similar rapid temperature fluctuations 4 cm above the rock surface (Fig. 2*C*), indicating that the warm-water events reached the bottom and that they were not highly localized on the scale of meters. The period of the bottom temperature fluctuations at ARP was 10.6 ± 5.4 min (mean ± SD, n = 36, from data in Fig. 2*C*). Every spike in bottom temperature was mirrored by a rapid increase in chlorophyll *a* concentration, on the order of 0.5–5.0 μg/liter, often matching the period of temperature fluctuations exactly. Bottom temperatures and chlorophyll *a* concentrations were highly correlated in all 12 of the CTD moorings, with Spearman's rank correlation coefficients ranging from 0.845 to 0.981. All correlation coefficients were significantly different from zero (all $P \leq 0.0001$; J.D.W., unpublished data).

Thermistor strings moored at the top of ARP for a total of 12 days revealed that many of the short-term temperature fluctuations recorded on the bottom were vertically coherent across the entire span of thermistors, which was 15 m in June and spanned 18–27 m in July (Table 1). Vertical coherence was quantified by correlation analysis to determine the degree of association between temperature records from different elevations above the bottom, for each thermistor string mooring. Temperature variability was positively correlated at all depths in June and July (Table 1). All correlation coefficients were highly significant; however, the strength of the correlation diminished with increasing vertical separation of the thermistors.

The simplest explanation for the large temperature and chlorophyll *a* spikes recorded on the bottom at ARP is that they were caused by rapid vertical displacements of the thermocline and the SCM layer associated with it to the bottom, as internal waves with amplitudes of 15–27 m passed over the pinnacle. This interpretation is supported by the significant correlations of temperature records across the water column to the bottom, establishing the vertical nature of the phenomenon, and by the amplitude and period of the bottom temperature fluctuations, which meet or exceed published accounts of temperature changes induced by internal waves [1.0–4.0°C in 6–8 min (16), 1.5–2.0°C in 10 min (18), 2.0–5.0°C in a few minutes (22)]. Further evidence that the temperature and chlorophyll pulses were induced by vertical motion associated with internal waves comes from observations of many alternating bands of slicks and rippled water at the surface above ARP on all calm days in June and July 1991 (15 out of 18 cruise days; J.D.W., unpublished data). Slicks are areas of convergence and downward circulation, representing the most obvious surface manifestation of internal waves (23, 24). A vertical CTD cast taken while anchored ≈80 meters south of ARP peak immediately before and during the passage of a northward moving slick revealed that the base of the thermocline and the depth of the chlorophyll maximum layer were vertically displaced by 25 and 18 m, respectively (Fig. 3).

Alternative Explanations. An alternative explanation for the large temperature and chlorophyll pulses recorded on the bottom is that they might have been caused by lateral advection of dense patches of phytoplankton in fronts or eddies moving past the pinnacle as the tide changes. According to this hypothesis, the causal mechanism would be a horizontal, rather than a vertical, process. A horizontal process would not explain the positive correlations between temperature and chlorophyll *a* established by the CTD/fluorometer moored at the top of the pinnacle, as the advected phytoplankton patch would be nearly isothermal with water at the peak. Nor would a passing front be likely to cause temperature changes on the same temporal scale as the

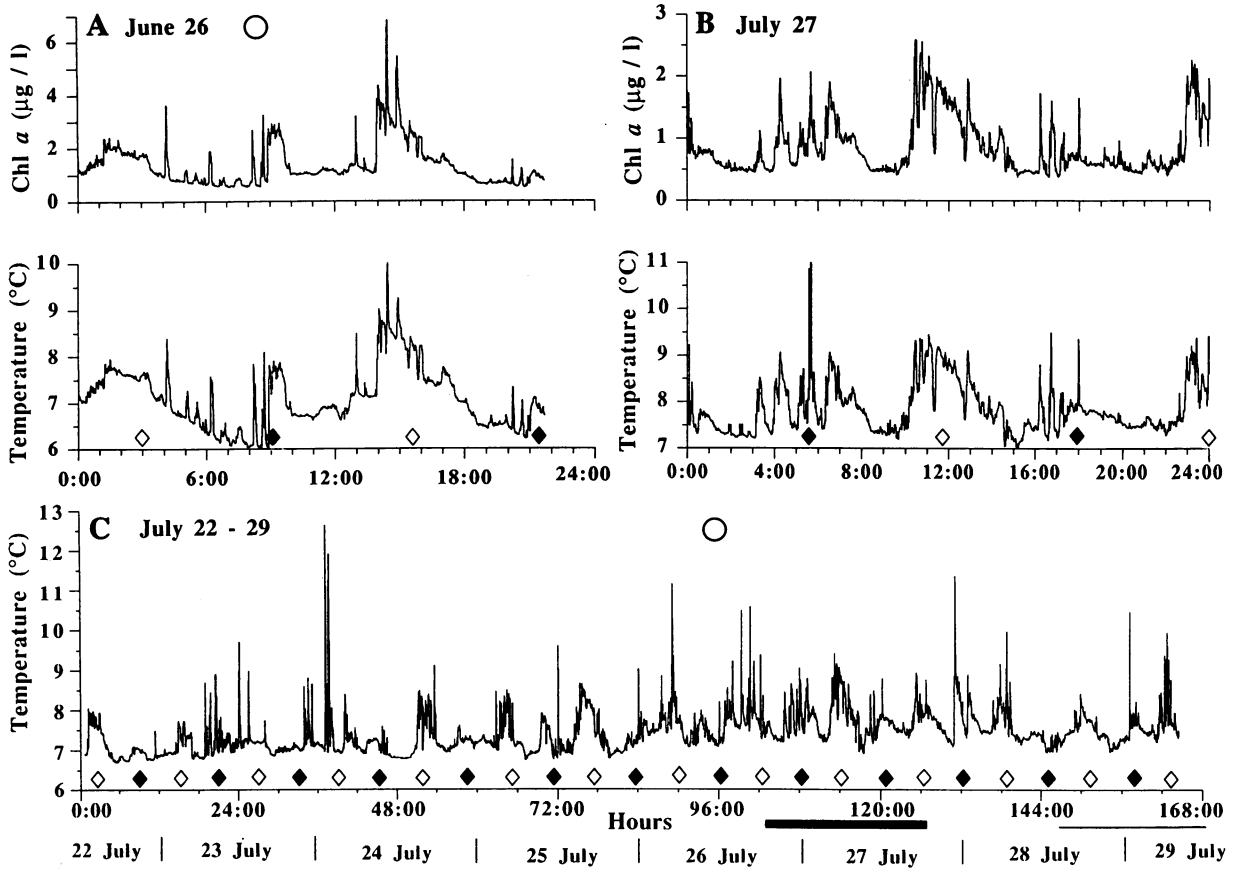

FIG. 2. Short-term fluctuations in chlorophyll *a* fluorescence and temperature at the peak (28-m depth) of ARP around spring tides [designated by full moon symbols (open circles) on June 26 and July 26]. Note the close correspondence between temperature and chlorophyll *a* recorded by the moored CTD/fluorometer in *A* and *B*; Spearman's rank correlation analysis indicated that temperature and chlorophyll *a* were highly correlated, with $r_s = 0.976$ in *A*, $r_s = 0.941$ in *B*. Each rapid temperature increase is accompanied by a 2- to 3-fold increase in chlorophyll *a* concentration. The 7-day record in *C* shows that rapid temperature increases are a characteristic feature of the peak site over the longer term. Open diamonds indicate time of low water, and solid diamonds designate time of high water; the flood tide begins ≈30 min before low water, and the ebb tide begins ≈30 min before low water. Thick bar indicates time of CTD record expanded in *B*; thin bar underlining end of temperature record in *C* indicates overlap of thermistor string mooring at south Cashes site (see Fig. 4) with the ARP record. These data indicate that the internal waves push the warm chlorophyll maximum layer right to the bottom, as the sensors of the CTD/fluorometer and the bottom thermistor in *C* were located 20 and 4 cm, respectively, above the rock surface.

high-frequency variation documented from 28 m (25, 26). Thus, the lateral-advection hypothesis has limited power to explain the observed phenomena. Wind-induced upwelling and downwelling are other mechanisms (27) deserving serious consideration, but since the majority of the measurements were taken on calm days with wind speeds below the critical threshold needed to generate Langmuir circulation [<3 m/sec (28) occurred on 15 of 18 days], wind-driven circulation could not be responsible for the dramatic temperature and chlorophyll changes observed on the bottom.

Mechanisms of Internal Wave Formation. Patterns of bottom temperature variability were studied to deduce the mechanisms of internal wave formation. Distinct ebb and flood tide patterns were evident, with the onset of ebb tide typically marked by a rapid temperature increase followed by a gradual decline to baseline levels (e.g., hours 14–20, 10–16, and 0–6 in Fig. 2 *A*, *B*, and *C*, respectively). By comparison, the temperature oscillations associated with the flood tide began a few hours before the flood and did not show the sudden jump to high temperatures and then a gradual decrease like the ebb tide. Instead, the flood-tide temperature changes were more like short warm-water pulses separated by a return to baseline (e.g., hours 8–9, 3–6, and 21–23 in Fig. 2 *A*, *B*, and *C*, respectively). Although the general pattern of temperature change differed between ebb and flood tides, analysis of temperature variability indicated that rapid temperature fluctuations characteristic of internal waves were equally likely on ebb and flood tides, occurring on 70% and 71% of the tides, respectively (Student's *t* test, $t = 0.013$, 1,44 df, $P > 0.05$, data arcsin transformed). Time-series analysis of the longest temperature record at the ARP site (Fig. 2*C*) resulted in a spectral density plot of temperature variance with two principal peaks at periods of 12.4 and 6.2 hr (plot available from J.D.W.). The first peak results from the prominent M_2 semi-diurnal internal tide (27). The second peak appears to be associated with the arrival of internal wave groups generated by the tides near the northern edge of Georges Bank, as described below. The wave packets arrive at the ARP site approximately at mid-phase of the local tide (Fig. 2), giving rise to the 6.2-hr spectral peak.

We hypothesize that there are two mechanisms controlling the striking temperature variation observed at ARP. The first is a "lee wave" wake forming behind the shallowest part of Cashes Ledge, Ammen Rock, located 5 km north of ARP (Fig. 1). As typical of lee waves elsewhere (11, 27), we suggest that the thermocline is depressed immediately downstream of Ammen Rock as the leading part of the internal wave train forms in the thermocline—hence the substantial increase in bottom temperature at ARP just after the ebbs begin. However, as the flow velocity of ebb tide increases, the lee-wave wake gets stretched out or pushed downstream, so that at ARP the thermocline relaxes slowly toward its

Table 1. Matrices of Spearman's correlation coefficients comparing temperatures measured once per minute at various depths during deployment of thermistor strings in 1991

June 25–27 (n = 2318)

	18 m	22 m	26 m	29 m
14 m	0.927	0.837	0.678	0.454
18 m		0.934	0.772	0.566
22 m			0.866	0.660
26 m				0.825

June 27–30 (n = 3958)

	18 m	22 m	26 m	29 m
14 m	0.854	0.599	0.425	0.404
18 m		0.791	0.560	0.454
22 m			0.814	0.582
26 m				0.749

July 10–11 (n = 1818)

	16 m	21 m	23 m	26 m	29 m
11 m	0.655	0.522	0.475	0.390	0.289
16 m		0.789	0.653	0.471	0.292
21 m			0.885	0.675	0.475
23 m				0.822	0.619
26 m					0.787

July 22–27 (n = 6545)

	8 m	12 m	18 m	29 m
1.5 m	0.426	0.270	0.184	0.285
8 m		0.850	0.705	0.281
12 m			0.858	0.286
18 m				0.269

July 28–29, south Cashes (n = 1495)

	6 m	9 m	15 m	22 m	29 m
2 m	0.590	0.353	0.221	0.210	0.133
6 m		0.809	0.633	0.575	0.418
9 m			0.796	0.695	0.485
15 m				0.867	0.675
22 m					0.876

The 29-m thermistor was located at the peak of ARP (except for the south Cashes site). All correlation coefficients are significantly different from zero at $P \leq 0.0001$.

mean level. Extensive current-meter data indicate that the ebb tide flows south over ARP (J.D.W., unpublished data), which is consistent with the lee-wave model. Three lines of evidence suggest that the distinct temperature oscillations occurring around the flood tide at ARP result from internal wave packets propagating into the study region from a distant source, probably from the northern edge of Georges Bank, where the transverse tidal currents generate energetic internal soliton packets that apparently propagate away from the bank into the Gulf of Maine. (*i*) Packets of internal waves have been depicted travelling northward from Georges Bank to Cashes Ledge by the sun glitter pattern in photographs taken from space (29). (*ii*) The predominant current direction recorded during large flood-tide temperature oscillations at ARP was from southeast to northwest (J.D.W., unpublished data), which is consistent with the direction of internal wave packets traveling from the northern margin of the shelf/slope break of Georges Bank. The propagation speed of these packets is about 120 km/day (29), meaning that they would arrive at ARP sometime around the flood tide 24 hr later because the site is 125 km away from the closest shelf/slope break on Georges Bank. Finally, internal wave signatures are more distinct during flood tides at the southern end of Cashes Ledge than on the study pinnacle (Fig. 4), as would be expected from northward-traveling packets of internal waves before they are disrupted by interaction with the abrupt bottom topography characteristic of the central region of Cashes Ledge.

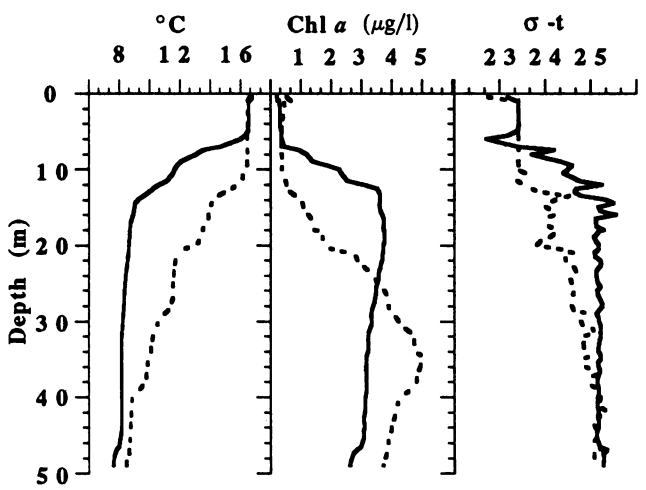

FIG. 3. Vertical profiles taken 80 m south of the peak of ARP on July 10, 1991, eleven minutes before (solid line) and during (dashed line) the passage of a large surface slick. The upper mixed layer was displaced 6 m downward, the bottom of the thermocline moved down from ≈12 to 39 m, and the depth of the chlorophyll (Chl) *a* maximum was displaced from 17 to 35 m as an internal wave traveled north toward the pinnacle. There was a sharp pycnocline between 6- and 14-m depth immediately before the slick, as shown on the density plot (far right; σ-τ, *in situ* density at atmospheric pressure). Brunt–Vaisala frequencies calculated from the density profiles ranged from 1.2 to 17 min, indicating that the density discontinuities are strong enough to support internal waves of the 8- to 30-min periods observed.

Concluding Remarks. In summary, we have identified a mechanism of food transfer from the water column to rocky subtidal habitats, and we have generated a testable hypothesis for the timing of internal waves on ebb and flood tides. The importance of this vertical coupling phenomenon as a source of food for suspension feeding invertebrates living on the bottom depends on the frequency of internal-wave downwelling, on the functional response of active and passive feeders to the pulsed food supply regime (30–32), and on the flow speed (33) and turbulence (34, 35) associated with food particle delivery. Based on our moored instrumentation (e.g., Table 1 and Fig. 2), we estimate that the SCM and thermocline are pushed down to the bottom by passing internal waves 8–20 times daily during the 6-month (May–October) period of thermal stratification in the outer Gulf of Maine. Thus, vertical coupling driven by internal waves should be a common and predictable mechanism of phytoplankton supply to the benthos. The functional response of suspension feeders to the variable food concentration, temperature, and flow conditions created by the pulsed downwelling of the SCM and thermocline is presently unknown. Clearly, it represents a rich area for further investigation. Previous growth experiments at the ARP site have shown that the growth rates of two species of facultatively active suspension feeders (36) were significantly greater at the top (28-m depth; the ascidian *Ascidia callosa*) or shallow slope (35 m, the encrusting bryozoan *Parasmittina*

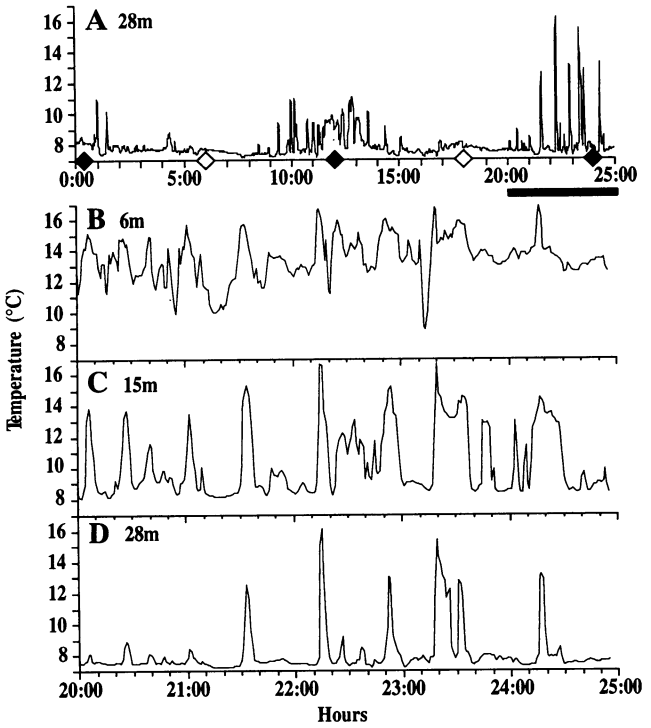

FIG. 4. Temperature variation 55 m above a nearly flat bottom 8 km south of ARP but at the same depth as ARP peak (28 m) from July 28 to July 29. A comparison of *A* and the last 24-hr period of Fig. 2*C* shows more distinct temperature variation around the 12.4-hr semidiurnal period of the internal tide at the south Cashes site, where the abrupt bottom topography of the pinnacle region has not distorted the internal wave field. *B–D* are expansions of the last 5 hr of *A* (underlined by solid bar) depicting a packet of internal waves with maximum amplitudes of 8°C and a typical duration of 8–12 min. Temperature variability is vertically coherent across the thermocline (6–28 m) and generally more coherent at south Cashes than at ARP, as indicated by higher temperature correlations between depths at the south Cashes site (Table 1).

jeffreysii) of ARP than at the deep slopes (50 m) of the pinnacle (J.D.W., unpublished data). Internal waves diminish with depth below the thermocline, and it is unlikely that waves with the amplitude described here commonly penetrate to 50 m. We suggest that increased phytoplankton supply brought about by the vertical displacement of the chlorophyll maximum layer is a compelling explanation for the high secondary production of facultatively active suspension feeders on the top and upper slopes of ARP and on other topographically high regions within the euphotic zone. Because the combination of steep bottom topography, thermal stratification, and vigorous tides needed to generate internal waves occurs in many temperate seas, this pulsed food supply mechanism should be applicable to subtidal habitats elsewhere.

We are indebted to divers E. Kintzing, T. Loher, G. Shellenbarger, D. Girouard, and W. Sutherland and the Nitrox dive supervisors at the National Oceanic and Atmospheric Administration's National Undersea Research Center at the University of North Carolina (Wilmington) for their invaluable help. The expert seamanship of the captains and crew of the R/V Cape Hatteras and the R/V Seward Johnson helped us achieve our research goals. We gratefully acknowledge D. Townsend's contribution to the investigation of SCM layers, and K. Sebens' assistance as the Director of the Marine Science Center. This research was supported by National Science Foundation Grant OCE-8800640, by the National Oceanic and Atmospheric Administration's National Undersea Research Center at the University of Connecticut (Avery Point); and by an equipment grant from the Max and Victoria Dreyfus Foundation. This is Marine Science Center contribution no. 197.

1. Smetacek, V. (1984) in *Coastal Oceanography*, NATO Advanced Research Institute, ed. Fasham, M. J. (Plenum, New York), Vol. 13, pp. 517–548.
2. Wishner, K., Levin, L., Gowing, M. & Mullineaux, L. (1990) *Nature (London)* **346**, 57–59.
3. Genin, A., Dayton, P. K., Lonsdale, P. F. & Spiess, F. N. (1986) *Nature (London)* **322**, 59–61.
4. Rowe, G. T. (1971) in *Fertility of the Sea*, ed. Costlow, J. D. (Gordon & Breach, New York), pp. 441–454.
5. Grebmeier, J. M., McRoy, C. P. & Feder, H. M. (1988) *Mar. Ecol. Prog. Ser.* **48**, 57–67.
6. Thorson, G. (1950) *Biol. Rev.* **25**, 1–45.
7. Apel, J. R. (1987) *Principles of Ocean Physics* (Academic, New York).
8. Halpern, D. (1971) *J. Mar. Res.* **29**, 116–132.
9. Apel, J. R., Holbrook, J. R., Liu, A. K. & Tsai, J. J. (1985) *J. Phys. Oceanogr.* **15**, 1625–1651.
10. Denman, K. L. (1977) *Limnol. Oceanogr.* **22**, 434–441.
11. Haury, L., Briscoe, M. G. & Orr, M. H. (1979) *Nature (London)* **278**, 312–317.
12. Haury, L. R., Wiebe, P. H., Orr, M. H. & Briscoe, M. G. (1983) *J. Mar. Res.* **41**, 65–112.
13. Grant, W. D. & Madsen, O. S. (1979) *J. Geophys. Res.* **84**, 1797–1808.
14. Brink, K. H., Jones, B. H., Van Leer, J. C., Mooers, C. N. K., Stuart, D. W., Stevenson, M. R., Dugdale, R. C. & Heburn, G. W. (1981) in *Coastal Upwelling*, ed. Richards, F. A. (Am. Geophys. Union, Washington, DC), pp. 473–495.
15. Genin, A. & Boehlert, G. W. (1985) *J. Mar. Res.* **43**, 907–924.
16. Witman, J. D. & Sebens, K. P. (1988) in *Benthic Productivity and Marine Resources of the Gulf of Maine*, eds. Babb, I. & DeLuca, M. (Natl. Undersea Res. Report, Rockville, MD), Vol. 88-3, pp. 45–66.
17. Witman, J. D. & Sebens, K. P. (1990) in *New Perspectives in Sponge Biology*, ed. Rutzler, K. (Smithsonian Inst. Press, Washington, DC), pp. 391–396.
18. LeFevre, J. (1986) *Adv. Mar. Biol.* **23**, 164–299.
19. Marra, J., Dickey, T., Chamberlin, W. S., Ho, C., Granata, T., Kiefer, D. A., Langdon, C., Smith, R., Baker, K., Bidigaire, R. & Hamilton, M. (1992) *J. Geophys. Res.* **97**, 7399–7412.
20. Townsend, D. W., Cucci, T. L. & Berman, T. (1984) *J. Plankton Res.* **6**, 793–802.
21. Morrison, M. A. & Townsend, D. W. (1988) *Hydrography and Vertical Plankton Distributions Over Rock Pinnacles in the Gulf of Maine* (Bigelow Laboratory for Ocean Sciences, West Boothbay Harbor, ME), Tech. Rep. 66.
22. Pineda, J. (1991) *Science* **253**, 548–551.
23. Apel, J. R., Byrne, M. H., Proni, J. R. & Charnell, R. L. (1975) *J. Geophys. Res.* **80**, 865–881.
24. Shanks, A. L. (1983) *Mar. Ecol. Prog. Ser.* **13**, 311–315.
25. Simpson, J. H. & Hunter, J. R. (1974) *Nature (London)* **250**, 404–406.
26. Denman, K. L. & Powell, T. H. (1984) *Oceanogr. Mar. Biol. Annu. Rev.* **22**, 125–168.
27. Bowden, K. F. (1983) *Physical Oceanography of Coastal Waters* (Horwood, Chichester, U.K.), pp. 124–184.
28. Mann, K. H. & Lazier, J. R. N. (1991) *Dynamics of Marine Ecosystems* (Blackwell Scientific, Cambridge, MA), pp. 267–273.
29. LaViolette, P., Johnson, D. R. & Brooks, D. A. (1990) *Oceanography* **3**, 43–49.
30. Koehl, M. A. R. (1977) *J. Exp. Biol.* **69**, 87–105.
31. Jorgensen, C. B. (1990) *Bivalve Filter Feeding: Hydrodynamics, Bioenergetics, Physiology and Ecology* (Olson & Olson, Fredensborg, Denmark).
32. Patterson, M. R. (1991) *Biol. Bull.* **180**, 81–92.
33. Vogel, S. (1981) *Life in Moving Fluids* (Princeton Univ. Press, Princeton, NJ).
34. Frechette, M., Butman, C. A. & Greyer, W. R. (1989) *Limnol. Oceanogr.* **37**, 19–36.
35. Shimeta, J. & Jumars, P. A. (1991) *Oceanogr. Mar. Biol. Annu. Rev.* **29**, 191–257.
36. LaBarbera, M. (1984) *Am. Zool.* **24**, 71–84.